2018 European Control Conference (ECC)
June 12-15, 2018. Limassol, Cyprus

Experimental validation of landing-gear dynamics for anti-skid control design

L. D'Avico[a], M. Tanelli[a] and S.M. Savaresi[a]

***Abstract*— Aircraft control systems are in general difficult to test in their final deployment phases, as flight time has very high costs and entails possible dangerous working conditions. Thus, coming to test flights with control algorithms that have been thoroughly tested beforehand is paramount. As far an anti-skid control is concerned, the industrial practice is to have the anti-skid controller embedded in the landing gear, so that the initial test bench for controller design is a rig comprising all or parts of the landing gear system. In this work, we extend a previously designed dynamic model of the landing gear with the experimental characterization of the hydraulic braking system. Then, a test-rig is setup, which allows testing the contact between wheel and ground with a flywheel. Open-loop experiments to tune the simulator are conducted, and a final validation of the simulation model against experimental data is carried out.**

I. INTRODUCTION

Active control systems are a very important part of modern aircraft. Besides flight controllers, which ensure autonomous capabilities, there are also many ancillary sub-systems that are dedicated to manage single functions. In this context, anti-skid control systems have been present on aircraft for many decades, being the precursors of those that were later designed for cars, [1]–[5]. In the current industrial practice, anti-skid systems are provided by braking systems suppliers as *black-boxes* that come with the actuation system, and which only need connection with the wheel speed sensor. They are directly installed in the landing gear, and in general do not communicate either with the other landing gear or with other parts of the aircraft, [6]. To design and test such systems, it is very important to rely on dynamic models which are as accurate as possible, because the final testing and tuning phases on the real aircraft must be limited due to high operational costs. Therefore, it is important to setup appropriate test rigs with a twofold aim: tune the design model accurately, and perform the initial tests of the control system.

This paper starts from the modelling of the single-corner dynamics, considering the common practice in ABS design from the automotive field (see *e.g.* [5], [7]). This model is expanded taking into consideration the peculiar effect that the gear-walk phenomenon has on the braking dynamics of aircraft, see [4]). Such a dynamic element must be taken into account in order to model the possible coupling that it may induce with the closed-loop anti-skid control logic.

*This work was supported by the Italian Ministry of Economic Development and Leonardo Aircraft Division within the cluster project TIVANO.

[a] L. D'Avico, M. Tanelli and S. M. Savaresi are with the Dipartimento di Elettronica, Informazione e Bioingegneria, Politecnico di Milano, Piazza Leonardo da Vinci 32, 20133 Milano, Italy.

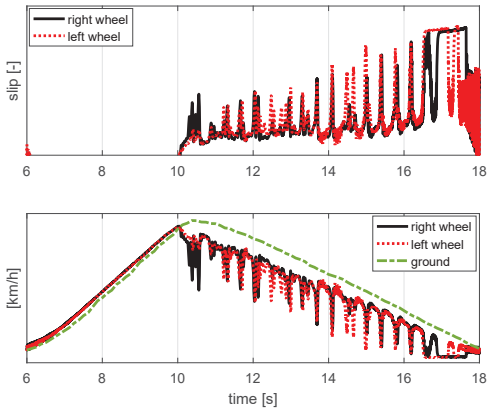

Fig. 1. Time histories of the wheel slip (top) and wheel and aircraft speed (bottom) measured in a rejected take-off braking manoeuvre with anti-skid control.

The vehicle model is then complemented with the hydraulic actuator dynamics, which is derived from experimental data. Further, a landing gear test rig has been setup for the initial controller tests. The main contribution of this paper is the calibration of the final non-linear landing gear model and its validation against the test rig experiments. Further, the final open-loop tests have been tuned to mimic the real behaviour of the wheel slip in current anti-skid braking maneuvers, both with standard and more advanced control algorithms, see [4]. For confidentiality reasons, the data from the experiments are shown omitting the axes scales.

The structure of this paper is as follows: Section II presents experimental data with real aircraft using anti-skid control to analyze the closed-loop signals. Section III introduces the description of the test rig set-up adopted to perform tests and collect experimental data, while Section IV discusses the mathematical non-linear model adopted to replicate the system in a simulation environment; Section V illustrates the simulation results comparing the simulation model with the experimental results.

II. ANALYSIS OF EXPERIMENTAL CLOSED-LOOP DATA

To investigate the typical behaviour of an aircraft during emergency braking, experimental data measured on small aircraft equipped with anti-skid systems was examined, based on tests carried out by Leonardo Aircraft Division on existing airplanes. For confidentiality reasons, data will be displayed omitting the y-axis scales.

In aeronautic anti-skid tests, two different manoeuvres are usually considered, namely a braking following a *landing*, and a braking due to an *rejected take-off* (RTO). The two differ in the braking intensity, as the latter has much more stringent constraints due to the limited length of runway available. The only measured variable in this systems is the wheel speed. In landing, a first phase of purely aerodynamic braking is experienced, after which the real controlled braking commences, and the anti-skid acts on the wheel slip to avoid wheels locking. The initial waiting phase allows the nose wheel, after the two landing gears touch the ground, to fully touch the ground too, as only after that event the braking system can safely be activated at full authority. In the RTO, instead, the aircraft is always on the ground, and thus the braking manoeuvre can be activated immediately after the take-off rejection is commanded. As for the wheel slip behaviour, the two manoeuvres show a similar pattern (in Figure 1 the behaviour in an RTO braking is shown): the anti-skid systems issues a series of opening and closing of the braking system valves to induce a sort of limit cycle on the wheel slip, the value of which should be kept away from locking and as close as possible to the peak of the (unknown) friction curve to improve performance.

Based on this analysis, one may see that the algorithm implemented by industrial anti-skid system is based on thresholds on the wheel deceleration, designed to obtain a limit cycle on the wheel slip in closed-loop. Such a design approach was used also in traditional ABS systems for cars, see *e.g.*, [8]–[10]. In more recent years, in the Automotive world braking systems have been designed as slip controllers, which can estimate the wheel slip and track a desired set-point obtaining a smooth transient with little or no oscillations, see *e.g.*, [5], [7], [11] and references therein. These two types of transients, *i.e.*, one with large and one with small oscillations on the wheel slip, will be used as reference to test the final validity of the final model against experimental data.

III. EXPERIMENTAL SET-UP

In the industrial design flow of anti-skid systems for aircraft, it is common to perform the initial tests on a test rig. The experimental tests presented in this work were also obtained on a test rig, which is shown in Fig. 2. Specifically, the rig is composed of: a flywheel, a landing gear, a moving sledge and a loading device used to simulate the vertical load acting on the tire.

To perform the tests, the flywheel is accelerated up to the desired initial speed for the landing manoeuvre; the landing gear is detached from the flywheel in this preliminary part. Afterward, the landing gear's sledge is moved forward to the flywheel to put the wheel in contact with the flywheel and to simulate the touch-down phase that takes place before the landing manoeuvre. After a first speed transient necessary to stabilize the wheel speed in proximity of the flywheel speed, the braking manoeuvre is started by applying the desired braking pressure profile. The loading device allows to simulate the load variation due to the presence of the lift force at different aircraft speed and the consequent compression of the tire radius (see also Section IV-B).

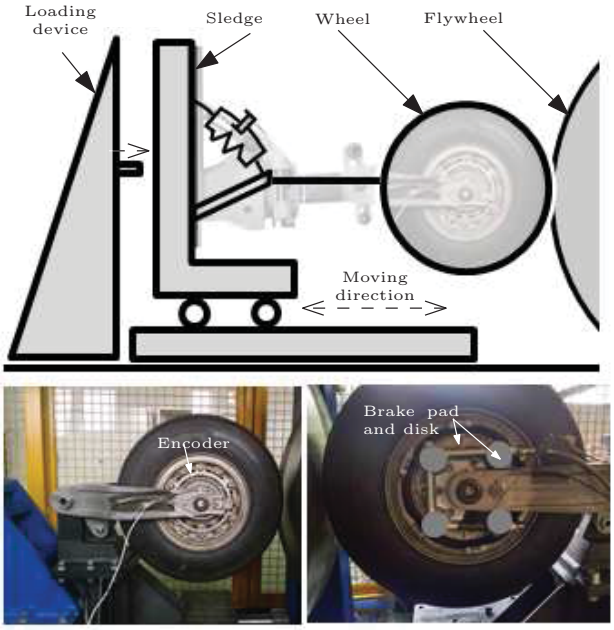

Fig. 2. Experimental set-up overview: [top] schematics of the landing-gear test rig; [bottom left] wheel encoder; [bottom right] brake pad and disk.

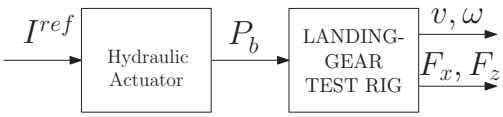

Fig. 3. Test rig: schematic overview of the experimental set-up.

The wheel and flywheel speed are measured using magnetic encoders, while a pressure sensor provides the measure of the braking pressure applied to the disk. Finally, the vertical load and the longitudinal force are measured by load cells. For the actuation of the braking pressure, an hydraulic actuator is used: a reference input current signal is imposed to obtain the desired braking pressure. The actuator dynamics are analysed in details in Section IV-C. For a clearer overview of the experimental set-up, in Fig. 3 the test rig and the main signals are represented as a block diagram.

IV. SYSTEM MODELLING

A. Introduction

To discuss the system model shown in Fig. 4, this section first presents the analysis of the non-linear model of the landing gear. Then, the modelling and experimental identification of the friction coefficient $\mu(\lambda)$ between the tire and the flywheel surface is addressed. Finally, the model is completed with the experimental identification of the actuator dynamics $A(s)$.

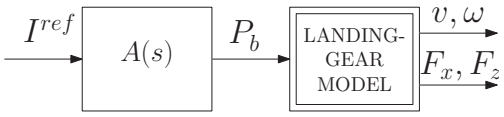

Fig. 4. Test rig block scheme: schematic overview of the system model.

B. Dynamic model of the landing gear

To obtain a control-oriented model of the landing gear, the wheel dynamics must be described, see also [4]. To this end, the wheel slip ratio can be defined as

$$\lambda = \frac{v_h - \omega r}{v_h}, \tag{1}$$

where v_h is the wheel hub speed, r is the wheel radius and ω is the angular wheel speed. The hub speed is defined as

$$v_h = v_a - \dot{\theta} L_{gw}, \tag{2}$$

where v_a is the aircraft longitudinal speed, $\dot{\theta}$ is gear walk angular speed and L_{gw} is the length of the link between the chassis and the wheel. Another important variable for control design is given by the normalized wheel deceleration η, defined as

$$\eta = -\frac{\dot{\omega} r}{g}, \tag{3}$$

where $\dot{\omega}$ is the wheel deceleration and g is the gravitational acceleration.

The tire-runway interaction is defined by the longitudinal force F_x as a function of the vertical load F_z and of the wheel slip defined as

$$F_x = F_z \mu(\lambda), \tag{4}$$

where $\mu(\lambda)$ models the road friction conditions, which will be discussed in detail later. In the modelling of the landing gear, a time-varying wheel radius is considered, as well as a varying vertical load, that takes into account the lift force. Such varying lift force induces modifications of the contact patch, which in turn explain the dynamic variations of the wheel radius, see [5], [8], [12].

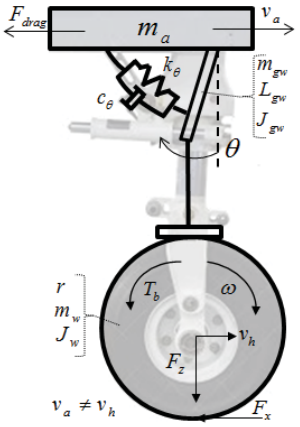

Fig. 5. Schematic representation of the control-oriented dynamic description of the aircraft landing gear.

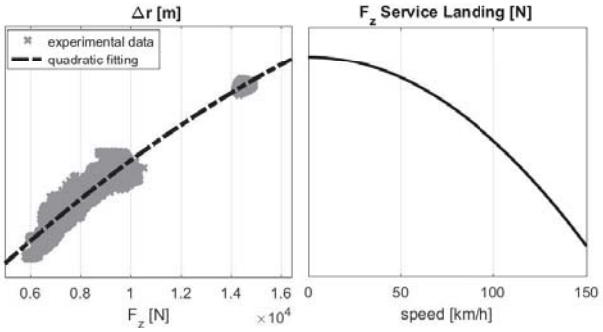

Fig. 6. [left] Static relationship between the tire compression and the vertical load; [right] Static relationship between vertical load and aircraft speed.

To our best knowledge, the combination of the gear-walk, suspensions and longitudinal motion has not been extensively studied in the aeronautic field from the anti-skid design point of view yet. In principle, the gear-walk motion can introduce a strong coupling between the longitudinal and vertical dynamics, so that it is very important to account for it in view of anti-skid design.

The non-linear model of the aircraft landing gear, which is schematically represented in Fig. 5, can be described as

$$(m_a + m_w + m_{gw})\dot{v}_a - J_\theta \ddot{\theta} = -F_x - F_{drag} \tag{5}$$

$$J_{\ddot{\theta}} \ddot{\theta} - J_\theta \dot{v}_a + c_\theta \dot{\theta} + k_\theta \theta = L_{gw} F_x \tag{6}$$

$$J_w \dot{\omega} = r F_x - T_b, \tag{7}$$

where $J_\theta = \left(\frac{L_{gw} m_{gw}}{2} + L_{gw} m_w\right)$, $J_{\ddot{\theta}} = \left(J_{gw+} \frac{L_{gw}^2 m_{gw}}{4} + L_{gw}^2 m_w\right)$ and $F_{drag} = \alpha_d v_a^2$ is the drag force. The value of the parameter α_d was tuned based on experimental data that are not reported here for sake of brevity. Notice that the measured input to the landing-gear system is given by the braking pressure, while the input of the non-linear model is the braking torque. For conversion purposes, the following expression can be employed

$$T_b = (\mu_b A_p R_{eff} n_s) P_b, \tag{8}$$

where μ_b is the friction coefficient between the pads and the brake disk, A_p is the total area of the pads, R_{eff} is the average distance between the pads and their point of application to the brake disk and n_s is the number brake disk surfaces involved in the braking manoeuvre, see [5], [13].

In Fig. 6 the static relationship between the wheel radius reduction (Δr) and the vertical load (F_z) is represented, showing both experimental data and its fitting using the quadratic function (the identified parameters values are omitted for confidentiality reasons).

$$\Delta r(t) = a F_z(t)^2 + b F_z(t) + c. \tag{9}$$

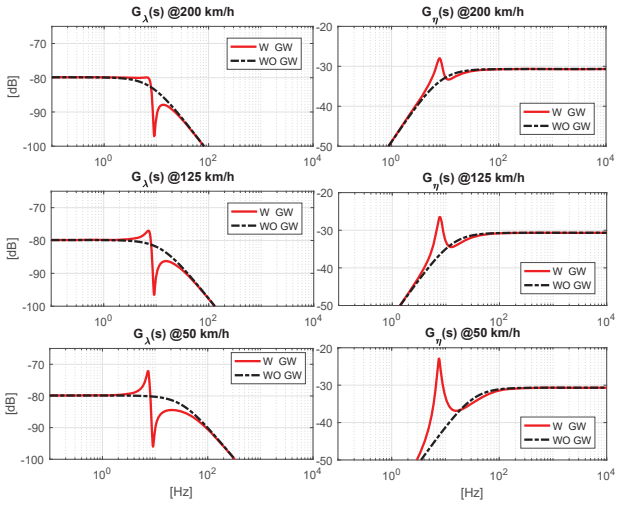

Fig. 7. Sensitivity of the frequency responses $G_\lambda(j\omega)$ and $G_\eta(j\omega)$ to different aircraft speed values, with (solid red line) and without (dashed-dot black line) the gear-walk dynamics.

Fig. 6 shows the static relationship between vertical load and aircraft speed, representative of a realistic braking manoeuvre on a runway; this static map is adopted to generate the reference force profile actuated by the loading device acting on the landing gear in the test rig (see Fig. 2).

The gear-walk phenomenon can be described as an oscillatory motion of the landing gear in the longitudinal direction, taking place around a static vertical center line. The main reason for this behavior is the coupling between the tire-runway friction condition modulated by the vertical load and the landing gear elasticity. It must be taken into account in the anti-skid design since it can be coupled with the anti-skid closed-loop control action (see *e.g.* [2]), with possible detrimental effects on the overall anti-skid performance. Such dynamics are compactly described as a rotational spring-damper.

For a quantitative analysis of the effects of the gear-walk phenomenon, the landing-gear model was linearized and the frequency responses associated to the transfer functions from braking torque to wheel slip ($G_\lambda(s)$) and from braking torque to normalized wheel deceleration ($G_\eta(s)$) were computed. For the sake of the clarity, Fig. 7 shows the comparison of the two frequency responses with and without the gear-walk dynamics, considering different – constant values – of aircraft speed. As can be seen, the landing-gear system without the rotational spring-damper modelling the gear-walk is essentially similar to the *single-corner* model taken from the Automotive world (see *e.g.* [5]). The description of the gear-walk causes the presence of a resonance at approximately 8[Hz], whose amplitude increases as the aircraft speed decreases.

C. Hydraulic actuator dynamics

The actuator dynamics (see block $A(s)$ in Fig. 4) are now modelled from experimental data by means of an appropriate identification procedure.

As first step, the static input/output relationship is investigated by means of tests carried out with a *quasi-static* input signal, *i.e.*, a sufficiently slow current ramp. The input current, the measured output pressure and the static current-pressure relationship obtained after the fitting are reported in Fig. 8. For the identification of the actuator dynamics the adopted procedure is depicted in Fig. 10 and 9, which show that step inputs were used together with sinusoids of varying frequency. Estimating the frequency responses from measured data and then fitting a parametric model, the transfer function representing the actuator dynamics was obtained as a second order model

$$A(s) = \hat{G}_{I^{ref}p}(s) = \mu \frac{\omega_n^2}{s^2 + 2\xi_n\omega_n s + \omega_n^2}. \qquad (10)$$

D. Friction curve $\mu(\lambda)$: modelling and identification

In the formulation expressed in 4, $\mu(\lambda)$ is the representation of the tire-road friction curve, and it describes the available friction available according to the different runway surfaces. Various empirical analytical expressions of $\mu(\lambda)$ were proposed in the literature. A widely-used expression (see *e.g.*, [5], [8]) is the so-called Burckhardt model, given by

$$\mu(\lambda) = \vartheta_1(1 - e^{-\lambda\vartheta_2}) - \lambda\vartheta_3, \qquad (11)$$

where the description of different road surfaces is obtained by varying the values of the parameters ϑ_i, $i = 1,2,3$.

For the experimental identification of the friction curve that models the interaction between the flywheel and the wheel in the test rig, several tests were performed: different input current steps were imposed to the hydraulic actuator to obtain braking maneuvers at constant pressure ranging from 5[bar] to 45[bar]. The high pressure area (up to 60[bar]) was not explored since the wheel skid event was observed at 45[bar]: thus, no further information could be retrieved

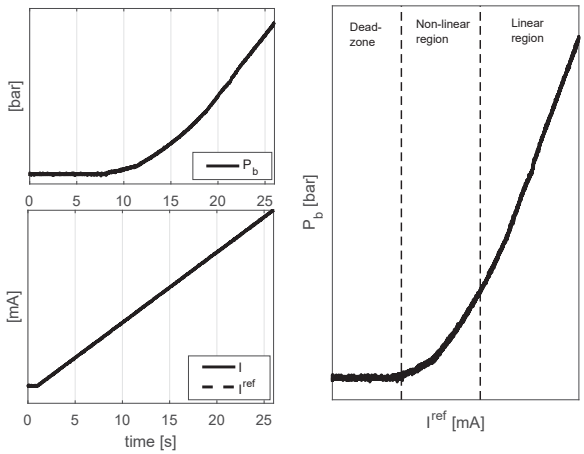

Fig. 8. Analysis of the static gain of the hydraulic actuator. Time histories of: [top-left] output pressure; [bottom-left] input current; [right] static current-pressure relationship

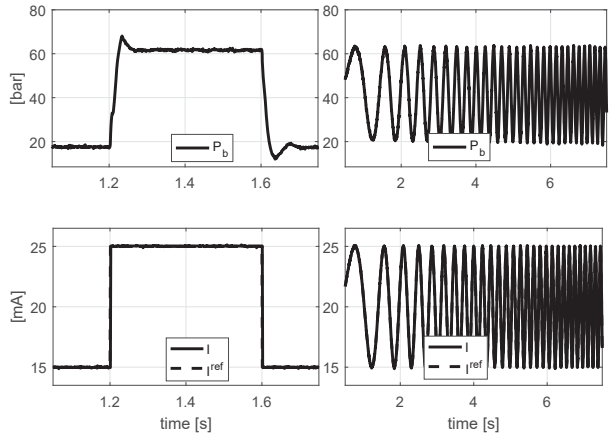

Fig. 9. Test input signals for the identification of the hydraulic actuator dynamics: [left] step, [right] sweep (with varying frequency 0.5Hz→100Hz)

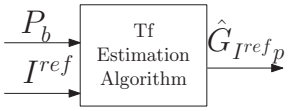

Fig. 10. Schematic procedure for the identification of the hydraulic actuator dynamics

for friction estimation purposes by increasing the braking pressure beyond this value.

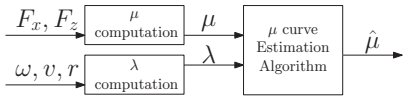

Fig. 11. Schematic representation of the identification of the friction coefficient $\mu(\lambda)$

The identification procedure is outlined in Fig. 11, which shows how the experimental data are used to obtain the wheel slip λ and the friction coefficient $\mu(\lambda)$. Specifically, the former is obtained exploiting the equality in (1), while the latter based on (4). These estimates are then used to obtain the experimental description of the flywheel friction curve by solving a non-linear curve fitting problem in least-squares sense, yielding the values of the coefficients $\vartheta_{1,2,3}$. The final results are shown in Fig. 12, where the quality of the final model can be appreciated. To better visualize the form of the experimental friction condition with respect to known ones, Fig. 12 offers a graphical and quantitative comparison, respectively, between the obtained values and the theoretical ones for dry and wet asphalt. Note that some differences between the theoretical and the experimental curves are present, the most relevant of which is that the final part of the experimental curve is much flatter than that of its theoretical counterparts. This is due to the fact that, with open-loop experiments, is very difficult to obtain points that explore the parameters' space beyond the peak of the curve, which correspond to open-loop unstable equilibria,

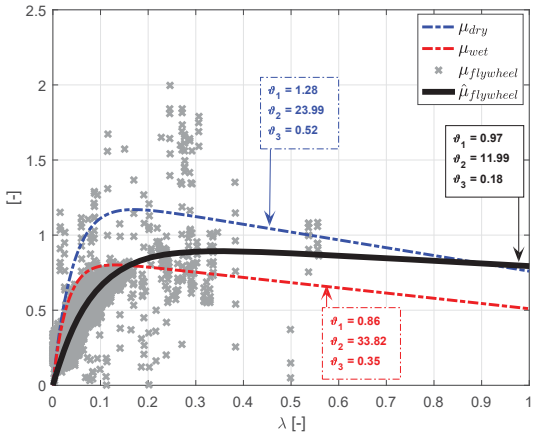

Fig. 12. Burckhardt curves - Experimental identification of the flywheel friction coefficient and comparison with dry and wet asphalt conditions

see [5]. As noted also in [13], this lack of precise modelling beyond, say, the value $\lambda = 0.5$, is not particularly meaningful for closed-loop control design, as also when using algorithms that induce closed-loop oscillations, the closed-loop system does not reach values of λ that go beyong this value. Should a more precise representation of the curve be needed, the approach outlined in [13] can be adopted, by fixing the value of ϑ_3 of (11) (which is responsible of the slope in the final part of the curve) in all conditions, and estimating only the remaining two parameters.

V. VALIDATION OF THE LANDING GEAR SIMULATION MODEL

To validate the landing gear dynamics model comprising the experimentally-identified actuator dynamics and the tire-road friction description, the experimental results obtained during real braking maneuvers on the test rig presented in Section III (see again Fig. 2,3)) are compared to the outputs obtained in simulation with the model described in Section IV (see also Fig. 4)). Fig. 13, 14a and 14b show a sample of the obtained results.

By inspecting Fig. 13, the accuracy of the overall identification procedure can be appreciated, showing that a suitable second-order transfer function $A(s)$ was identified to capture the static gain and the overall dynamics of the hydraulic actuator. The figure also shows a comparison between the braking pressure obtained experimentally (P_b) and the estimated one ($\hat{P}_b$) obtained simulating the the identified model $A(s) = \hat{G}_{I^{ref}p}(s)$, which can be seen as a validation of the identification results.

To perform the final tests in view of anti-skid design, we considered the typical profiles that the input current assumes when two different braking control algorithms are used, that were described in [4] and briefly described in Section II. Specifically, the two inputs have been designed to mimic the effects of a standard, threshold-based anti-skid controller as the one yielding the results shown in Figure 1, and another one imitating the behaviour of a pure slip controller.

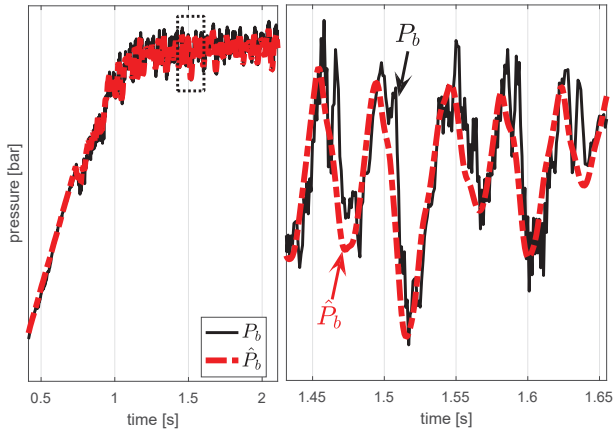

Fig. 13. Hydraulic actuator dynamics identification - [left] Validation of the identified model; [rigth] zoom of the figure on the left

Fig. 14a shows the results obtained in a test in which the reference current signal I^{ref} is modulated so that it oscillates with low frequency and rather high amplitude around the highest available current value (see Fig. 8) and this leads to remarkable oscillations on the wheel speed and on the wheel slip: also in this peculiar condition, the good agreement between the measured signals and the simulated ones is maintained.

Fig. 14b shows another test for the evaluation of the model accuracy, in which a different type of input signal I^{ref} was used. For a fair comparison with the previous test, the input current is limited again to its highest possible value, but now such value is modulated with oscillations at higher frequency and smaller amplitude. Such reduction in the oscillations of the input reference signal decreases the excitation of the system dynamics and generates a smoother profile of the wheel speed and of the wheel slip.

VI. CONCLUDING REMARKS AND OUTLOOK

In this work, a dynamic model of an aircraft landing gear developed initially based on first-principles was extended to comprise the experimental description of the actuation system and of the tire-road friction conditions available at the test rig. Satisfactory results have been obtained in terms of agreement between the measurements performed on the test rig and the simulations outputs after integration of all the estimated components. Ongoing work is dealing with the implementation of the anti-skid control algorithms on the test electronic control units in order to conduct the closed-loop testing phase.

ACKNOWLEDGMENTS

The authors aknowledge the work of Luca Bascetta, Marco Morandini and Gianluca Ghiringhelli, who realized the rig setup and assisted in the experimental activities.
The authors also want to acknowledge the constant support of M. Airoldi, A. Petrucci and G. Rapicano of Leonardo Aircraft Division.

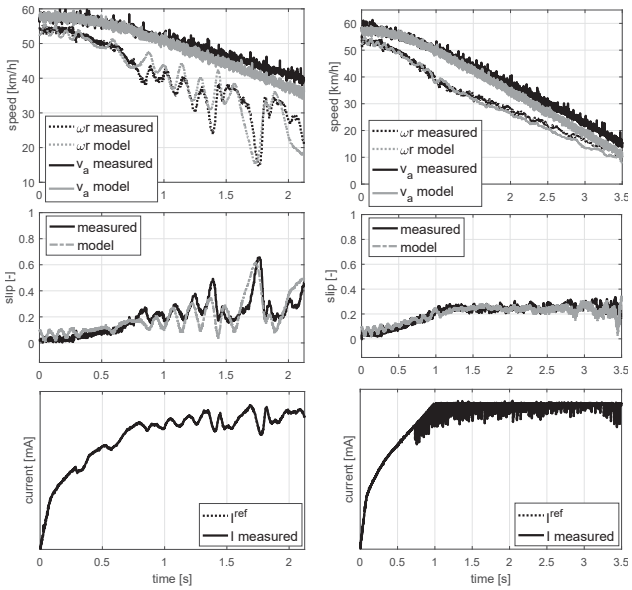

(a) (b)

Fig. 14. Landing gear braking maneuver: comparison between experimental measurements from the test rig and simulated results from the nonlinear model.

REFERENCES

[1] Robert Bosch GmbH, *Automotive Handbook, 7th Edition*. Wiley, New York, 2008.
[2] I. Tunay, "Antiskid control for aircraft via extremum-seeking," in *American Control Conference, 2001. Proceedings of the 2001*, vol. 2, 2001, pp. 665–670.
[3] S. Gualdi, M. Morandini, and G. L. Ghiringhelli, "Anti-skid induced aircraft landing gear instability," *Aerospace Science and Technology*, vol. 12, no. 8, pp. 627–637, 2008.
[4] L. DAvico, M. Tanelli, S. Savaresi, M. Airoldi, and G. Rapicano, "A deceleration-based algorithm for anti-skid control of aircraft," *IFAC-PapersOnLine*, vol. 50, no. 1, pp. 14 168 – 14 173, 2017. [Online]. Available: http://www.sciencedirect.com/science/article/pii/S2405896317327428
[5] S. M. Savaresi and M. Tanelli, *Active Braking Control Systems Design for Vehicles*. London, UK: Springer-Verlag, 2010.
[6] W. E. Krabacher, "Aircraft landing gear dynamics present and future," in *SAE Technical Paper*. SAE International, 1993.
[7] S. Savaresi, M. Tanelli, and C. Cantoni, "Mixed Slip-Deceleration Control in Automotive Braking Systems," *ASME Journal of Dynamic Systems, Measurement and Control*, vol. 129, no. 1, pp. 20–31, 2006.
[8] U. Kiencke and L. Nielsen, *Automotive Control Systems*. Springer-Verlag, Berlin, 2000.
[9] P. Wellstead and N. Pettit, "Analysis and redesign of an antilock brake system controller," *IEE Proceedings on Control Theory and Applications*, vol. 144, pp. 413–426, 1997.
[10] M. Tanelli, G. Osorio, M. di Bernardo, S. M. Savaresi, and A. Astolfi, "Existence, stability and robustness analysis of limit cycles in hybrid anti-lock braking systems," *International Journal of Control*, vol. 82, pp. 659–678, 2009.
[11] T. Johansen, I. Petersen, J. Kalkkuhl, and J. Lüdemann, "Gain-scheduled wheel slip control in automotive brake systems," *IEEE Transactions on Control Systems Technology*, vol. 11, no. 6, pp. 799–811, November 2003.
[12] R. Rajamani, *Vehicle Dynamics and Control*. New York: Springer, Mechanical Engineering Series, 2006.
[13] M. Tanelli, L. Piroddi, and S. M. Savaresi, "Real-time identification of tire–road friction conditions," *IET Control Theory and Applications*, vol. 3, no. 7, pp. 891–906, 2009.